ISSN 1068-3755, Surface Engineering and Applied Electrochemistry, 2017, Vol. 53, No. 5, pp. 439–448. © Allerton Press, Inc., 2017.

Corrosion Behavior of Severely Plastic Deformed Magnesium Based Alloys: A review[1]

D. Ahmadkhaniha[a], *, M. Fedel[b], M. Heydarzadeh Sohi[a], and F. Deflorian[b]

[a]*School of Metallurgy and Materials, College of Engineering, University of Tehran, Tehran, PO Box 1155-4563, Iran*

[b]*Department of Industrial Engineering, University of Trento, Trento, 38123 Italy*

**e-mail: ahmadkhany@ut.ac.ir*

Received May 23, 2016

Abstract—The purpose of this paper is to provide an overview of the impact of the microstructural modifications via severe plastic deformation on the corrosion behavior of magnesium and its alloys, especially when they are considered to be biodegradable materials. Mechanical processing involved in grain refinement modifies textures and residual stresses of materials which have their own impacts on corrosion behavior as reported in a large number of studies. However, the existing literature on the influence of microstructure on corrosion resistance is often contradictory, which discloses a lack of knowledge in this area. In this article the effects and contributions of critical factors such as the grain size, texture, residual stress and second phase distribution, affected by severe plastic deformation, on the magne-sium corrosion behavior is reviewed in order to find a relation between the microstructure and corrosion resistance.

Keywords: magnesium, corrosion, grain boundaries, texture, severe plastic deformation, biodegradable material

DOI: 10.3103/S1068375517050039

INTRODUCTION

Magnesium (Mg) and its alloys have received extensive attention as biodegradable implant materials in recent years. Magnesium is involved in many metabolic reactions and physiological mechanisms with recommended daily intake of 300–400 mg/day. It is also one of the most important bivalent ions in the formation of biological appetites in bone implants. It has further advantages over other implant materials due to its close density and Young's modulus to that of the natural bone. The major drawback of magnesium alloys is their poor corrosion resistance in the physiological pH (7.4–7.6) environment [1–3], thereby losing their mechanical integrity before the end of the required period for bone tissue healing [4–8]. Magnesium and its alloys degrade in aqueous environments via electrochemical reactions according to reactions (1) and (2):

$$Mg \rightarrow Mg^{2+} + 2e^{-}; \quad (1)$$

$$2H_2O + 2e^{-} \rightarrow 2OH^{-} + H_2. \quad (2)$$

The overall reaction is written as reaction (3).

$$Mg + 2H_2O \rightarrow Mg(OH)_2 + H_2. \quad (3)$$

The promising application of magnesium and its alloys as biodegradable materials depends on the ability of controlling their rates of corrosion in body fluids. Therefore, a lot of researchers have focused their efforts on the corrosion behavior of magnesium and its alloys in different solutions to commercialize biodegradable magnesium alloys [9–21]. Several methods have been proposed to protect magnesium against corrosion, such as magnesium purification [2], surface modifications and its coatings [22–28] as well as alloying with other elements [29–31]. Nevertheless, a procedure that can enhance corrosion resistance and mechanical strength simultaneously seems to be more beneficial. Mechanical processing involved in grain refinement usually raises mechanical strength and at the same time it can modify textures and residual stresses of materials that have their own impacts on corrosion behavior. It has been well established that mecha-nical processing such as rolling [32], equal channel angular pressing (ECAP) [33], friction stir processing (FSP) [34], high pressure torsion (HPT) [35] and extrusion [36] can enhance mechanical properties of magnesium alloys. So far, the effects of these processes on the corrosion resistance of magnesium alloys have been rarely studied. There are some review papers which provide an understanding on the type of corrosion and the ways of protection of magnesium alloys [37–40]. Although it has been shown that microstructure can alter the corrosion behavior of magnesium and its alloys [41–43], its impact has not been exactly cleared yet. In fact, in the case of magne-

[1] The article is published in the original.

Table 1. Summary of the grain refinement effect on corrosion resistance of Mg based alloys

Material	Processing route	Grin size, μm	Corrosion media	Corrosion test	Corrosion resistance	Reference
AZ31	HT, FSW	6–17	3.5% NaCl	PDP	Increased	[44]
Mg–Y–RE–Zr	HT	25	3.5% NaCl + $Mg(OH)_2$	PDP	Increased	[45]
Mg (99.9%)	HT, ECAP, SMAT	2–875	0.1 M NaCl	PDP	Increased	[46, 47]
AZ91	C	10–100	1 N NaCl	PDP	Increased	[42]
AZ91	C	15–100	3.5% NaCl	PDP and immersion	Increased	[48]
Mg (99.9%)	ECAP	2.6–125	0.1 M NaCl	PDP	Increased	[49]
AZ31	SPB	2.5	NaCl	PDP, EIS, H_2 evaluation	Increased	[50]
Mg–Zn–Ca	HPT	1.2	SBF	PDP	Increased	[51]
Mg–Nd–Zn–Zr	CEC	1	Hank's	pH monitoring, weight loss	Increased	[45]
Mg–4Li	HR	5	SBF	PDP	Increased	[32]
AZ31	ECAP	3–35	3.5% NaCl + $Mg(OH)_2$	PDP, EIS	Increased and decreased	[52]
WE43	E, ECAP	0.5–15	1% NaCl	Mass loss	Decreased	[53]
Pure Mg	SMAT	2.3	0.1 M NaCl	PDP	Decreased	[47]
Pure Mg	ECAP	50–100	3.5 wt % NaCl	Mass loss, EIS, PDP	Decreased	[54]
AZ91	ECAP	50–100	3.5 wt % NaCl	Mass loss, EIS, PDP	Decreased	[55]
Mg–1Ca	SMAT	6	Hank's	pH monitoring, H_2 evaluation, PDP	Decreased	[56]

HT: Heat Treatment, FSW: Friction Stir Welding, ECAP: Equal Channel Angular Pressing, SMAT: Surface Mechanical Attrition Treatment, C: Casting, SPB: Severe Plasticity Burnishing, HPT: High Pressure Torsion, CEC: Cyclic Extrusion and Compression, HR: Hot Rolling, E: Extrusion, PDP: Potentiodynamic Polarization, EIS: Electrochemical Impedance Spectroscopy.

sium alloys, the impact of micro-structural modifications by mechanical routes on corrosion behavior has not been well established yet. Since the capability to control the corrosion rate of biodegradable magnesium is a key-point for the design and development of efficient magnesium-based biodegradable implants, this review aims at providing an overview on the effect of the microstructure (i.e. grain size, texture, residual stresses, twinning, impurities segregation) on the corrosion behavior of magnesium and its alloys.

EFFECT OF GRAIN SIZE ON CORROSION

There are contradictory published data on the relationship of the grain size and the corrosion resistance, claiming that reducing the grain size value can variably increase or decrease corrosion resistance (Table 1). These contradictory results can be attributed to the underestimation of other microstructural changes that happen during mechanical processing applied on magnesium for structural refinement.

Grain size variation can be achieved by different conventional mechanical processing routes including rolling, forging, extrusion and inovative processes like ECAP, HPT and surface mechanical attrition treatment (SMAT). Apart from grain refinement, these processing routes change internal stresses, texture and second phase distribiution which can also affect the corrosion behavior. In addition, post processing and heat treatment can alter initially modified microstructure and make the interpretation of the results more complicated. It is, therefore, difficult to reach an unambiguous conclusion on the effect of the grain size on corrosion resistance.

It should also be noted that some of the contradictory reports are due to applying improper processing methods which induce non-homogenize strain and microstructure. For instance, poor corrosion resistance of extruded magnesium alloys has been reported [57] but it does not convey the adverse effect of grain refinement on corrosion resistance. As an example, extrusion results in a wide range of grain size value (Fig. 1a) due to non-homogenize strain. To eliminate this problem, modified processing routes such as cyclic extrusion and compression (CEC) [58] and double extrusion [59] have been examined which resulted in the formation of homogenous fine grain structure (Fig. 1b) and improved corrosion resistance (Fig. 1c).

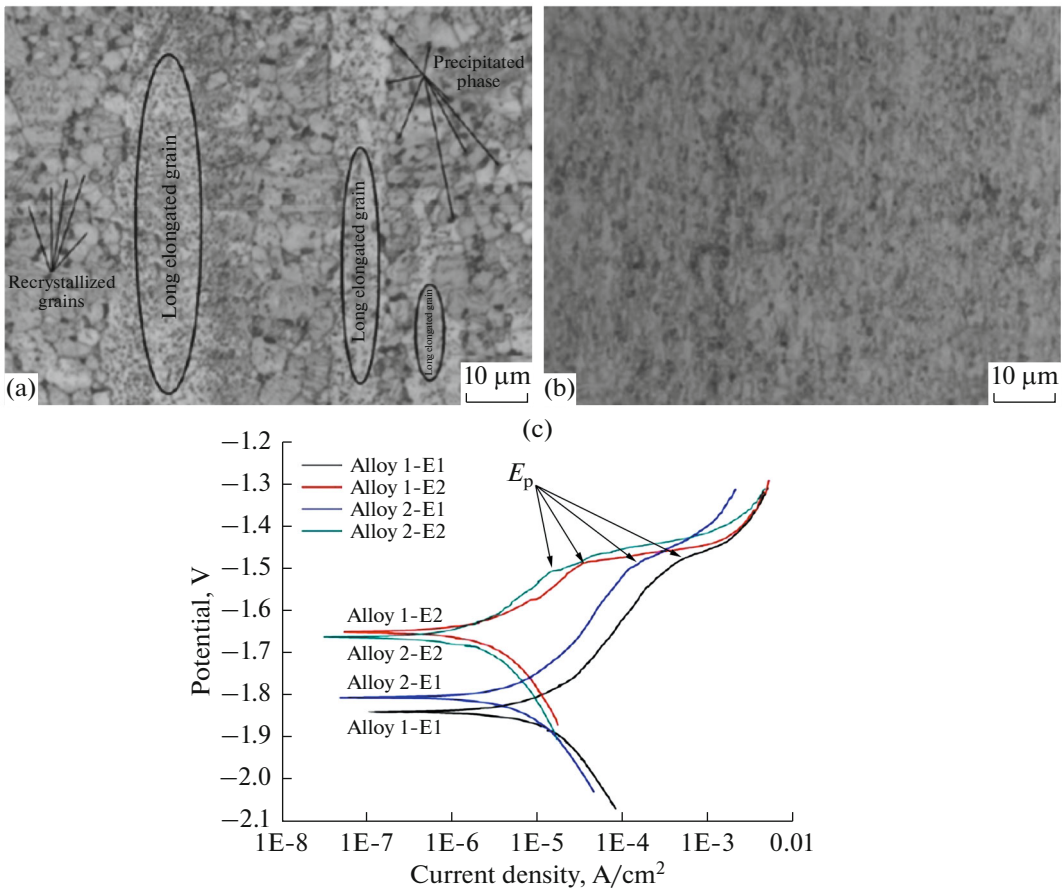

Fig. 1. (a) Microstructure of Mg–Nd–Zn–Zr alloys after single extrusion; (b) after double extrusion; (c) potentiodynamic polarization curves of Mg–Nd–Zn–Zr alloys after immersion in simulated body fluid for 1 h, alloy 1 is Mg–2.25 Nd–0.11 Zn–0.43 Zr and alloy 2 is Mg–2.70 Nd–0.20 Zn–0.41 Zr, alloys under single extrusion are denoted E1 and under double extrusion are denoted E2 [59].

In addition, the mass loss rate of as cast pure magnesium in 3.5% sodium chloride after being subjected to a number of ECAP treatments was measured in [54], whose authors reported that the corrosion rate increased with number of ECAP passes. However, the increase in corrosion rate was not related to the grain size reduction; it was mainly attributed to the surface pick up of iron containing particles in each ECAP pass [14].

The overall effect of grain boundaries can be summarized as follow. Grain boundaries increase the rate of diffusion and the electron activity and reduce atom coordination. Reducing atom coordination results in a lower work function of the surface, which makes removal and adsorption of species more feasible and probably increases rate of the charge transfer. Increased reactivity has also supported the notion that grain boundaries have adverse effect on corrosion resistance and function as initiation sites for corrosion. However, magnesium can be a special case since its oxide layer is not stable in aqueous solutions (The Pilling–Bedworth ratio for magnesium oxide is equal to 0.8) owing to high geometrical mismatch between the oxide layer and substrate. Additionally, the cubic magnesium oxide in aqueous solutions transforms to hexagonal magnesium hydroxide upon hydration, which has a volume approximately double of that of magnesium oxide. This process leads to disturbances in the film, causing compressive rupture which results in continual corrosion process. A fine-grained microstructure most likely provides a mean for relieving this stress via high fraction of grain boundaries and reduces the degree of oxide cracking [46, 47]. Hence, if the initial magnesium oxide layer formed on fine-grained surfaces provides better surface coverage and inhibits subsequent rupture of the exterior magnesium hydroxide layer, then slower corrosion rates in the case of fine-grained structures can be explained [46, 60].

Recently, some researchers [61, 62] have observed the formation of many isolated magnesium oxide nanocrystals on a fine-grained magnesium substrate under the magnesium hydroxide layer, which may have been formed by diffusion of oxygen atoms from the surface into the grain boundaries of the matrix. They assumed that the formation of this layer between

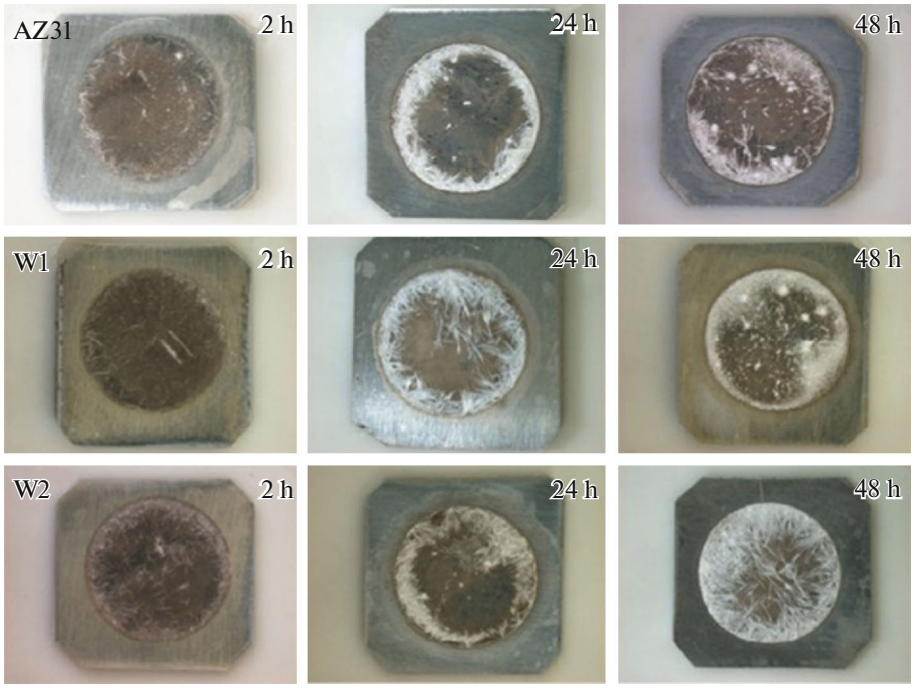

Fig. 2. The photo images of surface morphologies of the as-received AZ31, W1 and W2 (processed alloys) immersed in phosphate-buffered saline (PBS) solution for 2, 24 and 48 h. The as-received, W1 and W2 materials had an average grain size of ~ 20 μm, 2–6 μm and 0.72 μm, respectively [67].

the magnesium oxide layer and the magnesium substrate can decrease the sharpness of the tensile stress gradient across the interface and so the crack susceptibility of the magnesium oxide layer. In addition, grain boundary is well known as a place where impurities and solutes are dissolved. Some impurities and solutes act as effective cathodes, and accelerate the corrosion rate significantly; therefore, more grain boundaries means less detrimental impurities or precipitated solutes in the matrix, which enhances corrosion resistance [63].

The effect of grain boundaries also depends on the specific nature of the corrosion system. If corrosion progresses by active anodic dissolution, then grain boundaries will accelerate the corrosion rate. On the other hand, if the system undergoes passivation, then the grain boundaries will facilitate the passivation process and thereby reduce the corrosion rate. This behavior was confirmed in [41] via electrochemical impedance spectroscopy (EIS) measurements of fine and coarse grain structure immersed in a phosphate buffered solution (PBS). In this case, EIS measurements of fine grain samples showed a straight line associated with a diffusion process. This could be related to mass transport in the oxide layer due to the accelerated growth of the corrosion product layer as a result of the refined structure. In addition, a nobler open circuit potential (OCP) and higher breakdown potential value obtained for the fine grain samples as compared with the coarse structure, exhibited rapid formation of passive film on the refined structure [41]. On the contrary, more negative corrosion potential (E_{corr}) has also been reported for fine grain structures, as compared with those in the coarse ones [46, 64]. The corrosion potential is a consequence of anodic and cathodic reaction kinetics. It is mostly reported that grain refinement has the greatest influence on anodic reaction kinetic and can reduce it, therefore, E_{corr} becomes nobler [65, 66]. Nevertheless, if cathodic kinetics of the material decreases significantly, then the processing route that is used for grain refinement can be responsible for the overall reduction of E_{corr} [47].

Corrosion morphology of magnesium and its alloys depends on alloy composition and the environmental conditions as well as the grain size. For instance, an Mg alloy was processed by high-ratio differential speed rolling and the morphology of the phosphorous containing corrosion products on the surface of immersed processed samples in SBF changed by grain refinement. Different diameters and densities of the precipitates were achieved depending on the grain size of the substrate. The corrosion product layer formed on the surface of the fine structure was more compact than that of the coarse structure, as shown in Fig. 2 [67].

Furthermore, grain refinement modifies pitting behavior. It was found that preferred crystallo-graphic pitting (PCP) propagation reduced by refining the grain size of pure magnesium indicating that grain boundary acted as a barrier to pit propagation (Fig. 3) [68].

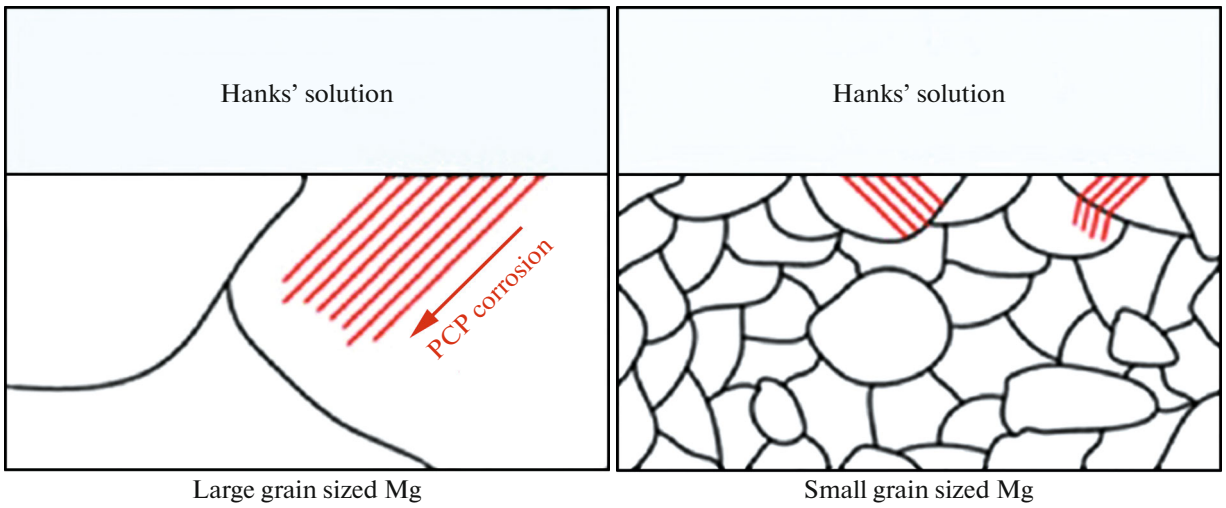

Fig. 3. Schematic diagrams showing the effect of grain refinement on limiting propagation of preferred crystallographic pits [68].

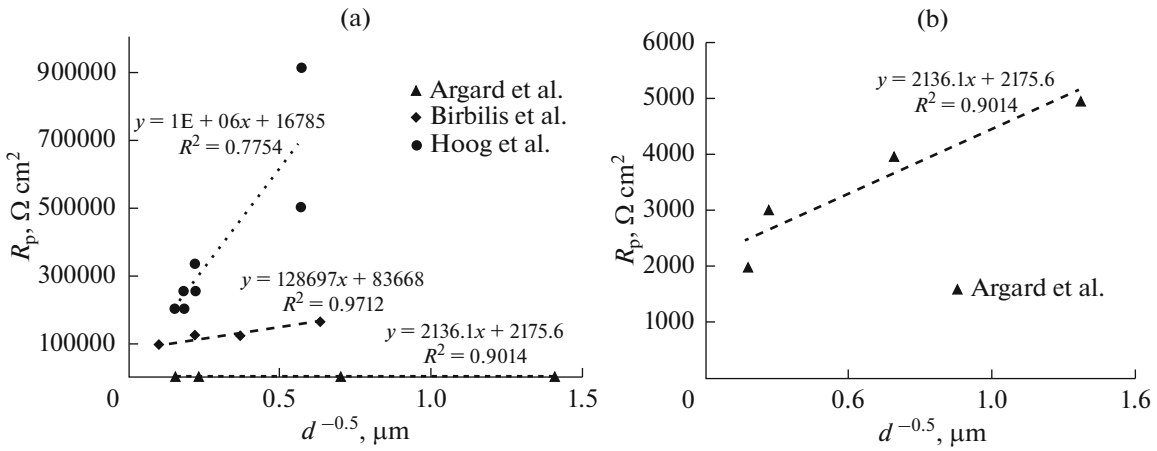

Fig. 4. R_p versus grain size for pure Mg and Mg alloy (a) in Birbilis et al., Hoog et al. and Argard et al. studies, (b) in Argard et al. study [49, 64].

It was also demonstrated that the type of corrosion could be varied from pitting to filiform depending on the processing used for modifying the structure [46]. Those researchers showed that the ECAP-treated sample with a lower corrosion rate was immune to the filiform type attack, and corroded eventually by only a pitting mechanism. The differences in corrosion morphology have not been studied deeply yet, but they highlighted the ability of the ECAP treatment to stifle the filiform attack.

Figure 4 shows the relation of the grain size (d) and polarization resistance (R_p) collected from different studies. In. [49], ECAP was used to refine pure magnesium and evaluate the corrosion rate in 0.1 M sodium chloride. In [64], the structure of magnesium alloy (Mg–Y–RE) by FSP was refined and the corrosion rate measured in the 3.5 wt % sodium chloride. In [47], SMAT was used to process pure magnesium as the base for the study of the corrosion behavior in 0.1 M sodium chloride. The author in [64] observed the relation between the polarization resistance and the grain size and their results are plotted separately in Fig. 4b.

The relationship observed in Fig. 4 in all cases is similar to Eq. (4) that reminds Hall–Petch equation.

$$R_p = A + Bd^{-0.5}, \quad (4)$$

where the constant A can be a function of the environment (since, the same material with a same grain size may have a different corrosion rate in different electrolytes) and B represents a material constant, which will differ according to the composition and the processing route employed to achieve grain refinement [64]. According to Fig. 4, the depen-dency of R_p on d (for pure Mg immersed in 0.1 M sodium chloride), is stronger in [47] than in [49]. This can be attributed to the impact of other microstructural parameters such

as texture, residual stress and twinning on corrosion resistance.

Considering the aforementioned data, it can be concluded that:

• Corrosion resistance of magnesium can be improved by homogenized structural refinement, which can accelerate the formation of the bilayer surface magnesium oxide and hydroxide (MgO + $Mg(OH)_2$). In addition, the mismatch stress between the surface layer and magnesium as well as pitting initiation can be reduced by grain refinement. The negative effect of impurities is also decreased by refining the grains.

• The relation between the grain size and polarization resistance approximately follows Hall–Petch equation.

EFFECT OF TEXTURE ON CORROSION

It is apparent that crystallographic texture has considerable impact on corrosion resistance. Crystallographic orientation and packing density influence reactivity and passive film formation. The corrosion resistance anisotropy in AZ31, dependent on crystallographic grain orientation, was discussed in [69, 70]. It was consistently confirmed that the rolled surface with (0001) plane has better corrosion resistance with a slightly thinner, but more compact, film than those in (101^{-}0) and (112^{-}0) planes in spite of having the similar grain size as shown in Fig. 5 [71]. A closely packed plane has a higher binding energy due to a higher atomic coordination, which lowers the surface energy.

In addition, the electrochemical dissolution rates of basal and prismatic planes calculated by Eq. (5) are different [69, 71].

$$I = nFk\exp\left(\frac{Q + \alpha nFE}{RT}\right), \quad (5)$$

where n is the number of electrons involved in the electrochemical reaction; k is a reaction constant; α is a transit coefficient; F, R, T and E are Faraday constant, gas constant, absolute temperature and the electrode potential, respectively. Q is the activation energy for a metallic ion to escape from the metal lattice and dissolve in the electrolyte solution, which is higher for the densely packed surfaces than those in the loosely packed ones.

The closely packed (0001) surface showed a more positive OCP value than that of less densely packed (101^{-}0) and (112^{-}0) ones. Different obtained OCPs imply the formation of microgalvanic cells between grains with different orientations [71, 72].

The surface energy has indirect, hence less significant, influence on the activation energy of hydrogen reaction than that for metal dissolution. Therefore, the difference between planes is less at the cathodic current density than at the anodic one [71].

It has been revealed [65, 73] that initiation and propagation of the localized attacks are crystallographic dependence. The magnesium (0001) surface revealed pitting corrosion susceptibility at the open circuit potential. While the (101^{-}0), and(112^{-}0) surfaces remained passive at OCP, pitting corrosion was initiated at slightly anodic potentials to their OCP. The critical pitting potentials for the magnesium single crystals increased in the order (0001), (101^{-}0), (112^{-}0), respectively [73]. A dependence of pitting on crystallographic orientation for magnesium has been also reported in [65], showing that pits nucleate on basal {0001} planes, but have a higher propagation rate along prismatic (101^{-}0) planes. With random crystal orientations, the corrosion current increased, but still remained lower than that on the (101^{-}0) planes. It should be noted that the difference between various crystallographic planes diminished after a short time heat-treatment; while heat-treatment did not change the grain orientation. Particularly, after heat-treatment more intermetallic phases precipitated and grew in the matrix. The authors in [69] shower that after heat-treatment, the amounts of the intermetallic particles increased more significantly on the basal surface than on (101^{-}0) and (112^{-}0) surfaces. This is led to a higher corrosion rate in the basal surface in comparison with other planes, which offsets the original difference in corrosion behavior between these surfaces. Different precipitation behaviors can be associated with various diffusion rates of elements and phase transformations along the basal and the prismatic planes. The interval between adjacent (0001) basal planes of the magnesium matrix phase is much larger than that of the prismatic planes [64]. There is more space along the (0001) planes for the formation and growth of precipitates. The best corrosion resistance of Mg–Ca alloy obtained after annealing, in spite of the sharp reduction in the maximum intensity of basal texture, was discussed in [74]. Apart from heat treatment, corrosion media can also affect the impact of texture. For instance, in a strong passivating or less aggressive solution, the difference between films formed on different grains is eliminated and therefore, reduces the grain orientation effect on corrosion performance [71].

To sum up it is necessary to say that the basal texture as a result of lower tendency for pits growth and lower dissolution rate is more resistant in corrosive environment. It was mentioned previously that there was not any sign of filiform corrosion on the surface of ECAP-treated magnesium which had a better corrosion resistance than coarse grained magnesium. Filiform corrosion can happen when pits grow laterally and join each other. Since the growth rate of pits is lower on the basal plane, therefore, filiform corrosion probability can be reduced by dominating basal texture through ECAP.

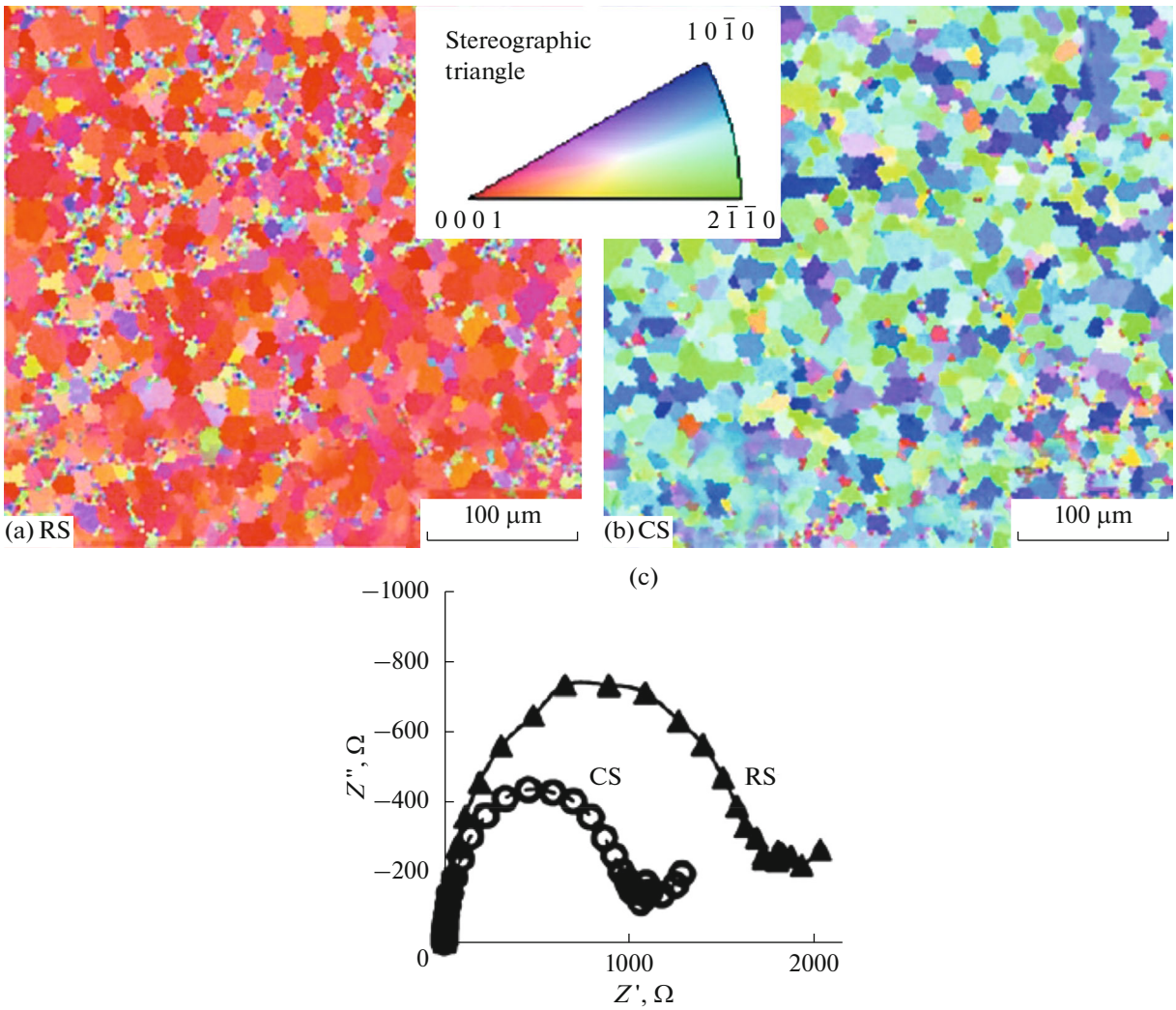

Fig. 5. Optical images of the microstructures of (a) the rolling surface (RS) with basal texture; (b) cross section (CS) of AZ31 sheet with the same grain size value (c) AC impedance spectra of the RS and CS surfaces in 5 wt % NaCl solution [71].

EFFECT OF RESIDUAL STRESS ON CORROSION

The underlying stresses and strains induced by processing may impart cracks or defects in the material and diminish any positive effect from increasing grain boundary densities. Residual stress will alter the free energy state of the material, which, in turn, can change the work function of the material surface. Micro scale residual stresses can decrease the activation energy for an atom to escape from the metal lattice and get into the solution. According to [75], the influence of the residual stress, as a result of burnishing, appears only in the anodic current densities during polarization tests. It was also demonstrated that tensile residual stress was unfavorable for the corrosion performance of AZ31B. On the contrary, the high compressive residual stress generated in the subsurface by a deep rolling process reduced the corrosion rate of Mg–Ca alloys [76].

EFFECT OF TWINNING ON CORROSION

Deformation twin is one of the noticeable defects in the magnesium alloys. Although the energy of a twin depends on its orientation relationship, it is known that atoms in the twin lattice are more active than in a normal crystallographic plane. In [77] it was shown that despite grain refinement induced by forging, the corrosion resistance of Mg–1Ca reduced due to the increase in the number of twinning planes. As a result of a high density of twinning and dislocation, anodic polarization behavior changed. Un-twinned samples exhibited self-passivation characteristics, while the twinned ones presented active dissolution in the electrolyte. Furthermore, the cathodic process is remarkably accelerated by twinning [78].

A survey in [79] indicated that the effect of grain size was less pronounced in the corrosion of the twinned microstructure. Twins further accelerated the intra-granular corrosion. On the contrary, the

researchers in [80] reported that twinned magnesium has better corrosion resistance than un-twinned one, which was attributed to the different behaviors at the early stages of the corrosion. They believed that in the case of the un-twinned magnesium alloy, at the beginning stage of the corrosion, the solution touched with the surface of the magnesium alloy and formed an interface directly. An oxide film is then produced beneath the interface, with prolonging the immersion time. Finally, some microcracks and pitting dots are formed, resulting in the continuous corrosion. For the twinned magnesium alloy, a homogeneous oxide film can be formed immediately at the initial stage of immersion test or polishing process which hinders corrosion process. Meanwhile, the fully coherent twin boundaries have lower interfacial energies with respect to those in the incoherent interfaces of grain boundaries [81]. Therefore, microcracks, formed due to the inhomogeneous orientation stress, mainly occur in grain boundaries rather than in twins and microcracks propagation inhibited by twins [80, 82]. Nevertheless, the literature in this aspect is limited; further research and investigations in this area are necessary to clarify the role of twins in corrosion resistance.

EFFECT OF SECOND PHASE AND IMPURITY SEGREGATION ON CORROSION

Based on the literature [30, 36, 43], alloying of magnesium may affect the corrosion response of the material two fold. Firstly, alloying additions can alter alloy chemistry, which gives rise to a different corrosion response. Secondly, the impact of alloying upon the microstructure influences both the corrosion kinetic and morphology, which depends on the relative solubility of the elemental additions in the magnesium matrix, and on the density, size and type of intermetallic that can be formed.

Segregation of impurities may make an alloy more susceptible to a localized intergranular attack. Furthermore, the presence of certain elements can even disturb the formation of a protective oxide [30]. Mechanical processing due to the induced strain is able to fracture second phases and distribute them uniformly in the alloy. The uniformly distributed tiny second phase usually can reduce the activity of galvanic corrosion. The processed structure with a large number of nano-sized second phase particles precipitated in the grain interiors without precipitation of the second phase at grain boundaries results in uniform corrosion with respect to the samples with the continuous second phase placed at the grain boundaries and micro-sized second-phase particles within the grain [83–87]. On the contrary, Mg–Al intermetallics (β-phase) in AZ alloys exhibited different behaviors. It is well established that the β-phase in AZ alloys plays a dual role. It can act either as a barrier or as a galvanic cathode. The β-phase has a barrier role when its fraction is not too low and nearly continuous over the small grain size magnesium matrix. While, discontinues distribution of β phase which is achieved by mechanical processing, results in the formation of a ''galvanic cathode'' and accelerates the corrosion rate of magnesium [43].

This contrary effect of the second phase distribution on corrosion can be explained by the role of the second phase as anode or cathode. In Mg–Ca alloy, it was observed that corrosion continuously dissolved Mg_2Ca phases (which acted as anode) and penet-rated along grain boundaries, resulting in acceleration of pitting corrosion. This circumstance is opposite to the observed effects in Mg–Al alloys, where $Mg_{17}Al_{12}$ phase (β phase) acts as cathode [36, 88].

Apart from size and distribution of the precipitations, their interfaces with the matrix play an important role. The transition from coherent precipitate to incoherent one alters the precipitate-matrix coherency strain in the matrix, which is equivalent to the micro-level stress relieving of the matrix and can change the corrosion behaviors [89].

CONCLUSIONS

In this review the effect of mechanically processed microstructure on the corrosion resistance of magnesium-based alloys has been reported and it was shown that:

• Grain refinement can improve corrosion resistance by dissolution of impurities and accele-rating passivity of magnesium alloys.

• Competition between initiation and propagation of pits, besides the electrochemical dissolution rate, determines the influence of different crystallographic planes on corrosion resistance.

• There are contradictory opinions about the effect of twinning on corrosion behavior of magnesium alloys.

• The effect of the second phase distribution, induced by mechanical processing, on corrosion behavior depends on the role of the second phase as anode or cathode.

On the whole, it appears that mechanical processing which results in a refined structure with dominant basal texture and minimum compressive residual stress can be a promising route for improving corrosion resistance of pure Mg.

REFERENCES

1. Song, G. and Song, S., *Adv. Eng. Mater.*, 2007, vol. 9, p. 298.
2. Song, G., *Corros. Sci.*, 2007, 49, p. 1696.
3. Wang, H., Estrin, Y., and Zúberová, Z., *Mater. Lett.*, 2008, vol. 62, p. 2476.
4. Müllera, W.D., Nascimento, M.L., Zeddiese, M., and Córsicoc, M., *Mater. Res.*, 2007, vol. 10, p. 1.

5. Manivasagam, G. and Dhinasekaran, D., *Corros. Sci.*, 2010, vol. 2, p. 40.
6. Witte, F., *Acta Biomater.*, 2010, vol. 6, p. 1680.
7. Staigera, M.P., Pietaka, A.M., Huadmaia, J., and Dias, G., *Biomaterials*, 2006, vol. 27, p. 1728.
8. Erlin, Z. and Lei, Y., *Mater. Sci. Eng., A*, 2008, vol. 497, p. 111.
9. Ascencio, M., Pekguleryuz, M., and Omanovic, S., *Corros. Sci.*, 2014, vol. 87, p. 489.
10. King, A.D., Birbilis, N., and Scully, J.R., *Electrochim. Acta*, 2014, vol. 121, p. 394.
11. Song, G., Atrens, A., Stjohn, D., Nairn, J., et al., *Corros. Sci.*, 1997, vol. 39, p. 855.
12. Jamesh, M.I., Wua, G., Zhao, Y., McKenzie, D.R., et al., *Corros. Sci.*, 2015, vol. 91, p. 160.
13. Song, Y., Shan, D., Chen, R., Zhang, F., et al., *Mater. Sci. Eng., C*, 2009, vol. 29, p. 1039.
14. Atrens, A., Liu, M., and Abidin, N.I.Z., *Mater. Sci. Eng., B*, 2011, vol. 176, p. 1609.
15. Song, G.L. and Atrens, A., *Adv. Eng. Mater.*, 1999, vol. 1, p. 11.
16. Winzer, N., Atrens, A., Song, G., Ghali, E., et al., *Adv. Eng. Mater.*, 2008, vol. 7, p. 659.
17. Winzer, N., Atrens, A., Dietzel, W., Raja, V.S., et al., *Mater. Sci. Eng., A*, 2008, vol. 488, p. 339.
18. Witte, F., Hort, N., Vogt, C., Cohen, S., et al., *Curr. Opin. Solid State Mater. Sci.*, 2008, vol. 12, pp. 63–72.
19. Kirkland, N.T., Birbilis, N., and Staiger, M.P., *Acta Biomater.*, 2012, vol. 8, p. 925.
20. Mueller, W.D., Nascimento, M.L., and Lorenzo de Mele, M.F., *Acta Biomater.*, 2010, vol. 6, p. 1749.
21. Virtanen, S., *Mater. Sci. Eng., B*, 2011, vol. 176, p. 1600.
22. Chiu, K.Y., Wong, M.H., Cheng, F.T., and Man, H.C., *Surf. Coat. Technol.*, 2007, vol. 202, p. 590.
23. Hornberger, H., Virtanen, S., and Boccaccini, A.R., *Acta Biomater.*, 2012, vol. 8, p. 2442.
24. Wang, Y., Wei, M., and Gao, J., *Mater. Sci. Eng., C*, 2009, vol. 29, p. 1311.
25. Xu, L., Pan, F., Yu, G., Yang, L., et al., *Biomaterials*, 2009, vol. 30, p. 1512.
26. Wu, C., Wen, Z., Dai, C., Lu, Y., et al., *Surf. Coat. Technol.*, 2010, vol. 204, p. 3336.
27. Li, H., Li, Z.X., Li, H., Wu, Y.Z., et al., *Mater. Des.*, 2009, vol. 30, p. 3920.
28. Wang, Q., Tan, L., Xu, W., Zhang, B., and Yang, K., *Mater. Sci. Eng., B*, 2011, vol. 176, p. 1718.
29. Zhang, S., Zhang, X., Zhao, C., Li, J., et al., *Acta Biomater.*, 2010, vol. 6, p. 626.
30. Gu, X.N., Xie, X.H., Li, N., Zheng, Y.F., et al., *Acta Biomater.*, 2012, vol. 8, p. 2360.
31. Zhang, E., Yang, L., Xua, J., and Chen, H., *Acta Biomater.*, 2010, vol. 6, p. 1756.
32. Nene, S.S., Kashyap, B.P., Prabhu, N., Estrin, Y., and Al-Samman, T., *J. Alloy Compd.*, 2014, vol. 615, p. 501.
33. Mostaed, E., Hashempour, M., Fabrizi, A., Dellasega, D., et al., *J. Mech. Behav. Biomed. Mater.*, 2014, vol. 37, p. 307.
34. Feng, A.H., Xiao, B.L., Ma, Z.Y., and Chen, R.S., *Metall. Mater. Trans. A*, 2009, vol. 40, p. 2447.
35. Edalati, K., Yamamoto, A., Horitaa, Z., and Ishihara, T., *Scr. Mater.*, 2011, vol. 64, p. 880.
36. Han, S.H., Minghui, Y., Kwang, S.H., Young, B.J., et al., *Mech. J. Behav. Biomed. Mater.*, 2013, vol. 20, p. 54.
37. Song, G. and Atrens, A., *Adv. Eng. Mater.*, 2003, vol. 5, p. 837.
38. Song, G., *Adv. Eng. Mater.*, 2005, vol. 7, p. 563.
39. Kirkland, N.T., Lespagnol, J., Birbilis, N., and Staiger, M.P., *Corros. Sci.*, 2010, vol. 52, p. 287.
40. Wei Guo, K., *Recent Pat. Corros. Sci.*, 2010, vol. 2, p. 13.
41. Alvarez-Lopez, M., Dolores Pereda, M., del Valle, J.A., Lorenzo de Mele, M.F., et al., *Acta Biomater.*, 2010, vol. 6, p. 1763.
42. Wang, H., Estrin, Y., Fu, H., Song, G., et al., *Adv. Eng. Mater.*, 2007, vol. 9, p. 967.
43. Song, G., Atrens, A., and Dargusch, M., *Corros. Sci.*, 1999, vol. 41, p. 249.
44. Jang, Y.H., Kim, S.S., Lee, C.G., and Kim, S.J., *Corros. Eng. Sci. Technol.*, 2007, vol. 42, p. 119.
45. Ben-Hamu, G., Eliezer, D., Shin, K.S., and Cohen, S., *J. Alloy Compd.*, 2007, vol. 431, p. 269.
46. Op't Hoog, C., Birbilis, N., and Estrin, Y., *Key Eng. Mater.*, 2008, vol. 384, p. 229.
47. Op't Hoog, C., Birbilis, N., and Estrin, Y., *Adv. Eng. Mater.*, 2008, vol. 10, p. 579.
48. Ambat, R., Aung, N.N., and Zhou, W., *Corros. Sci.*, 2000, vol. 42, p. 1433.
49. Birbilis, N., Ralston, K.D., Virtanen, S., Fraser, H.L., et al., *Corros. Eng. Sci. Technol.*, 2010, vol. 45, p. 224.
50. Pu, Z., Song, G.L., Yang, S., Outeiro, J.C., et al., *Corros. Sci.*, 2012, vol. 57, p. 192.
51. Gao, J.H., Guan, S.K., Ren, Z.W., Sun, Y.F., et al., *Mater. Lett.*, 2011, vol. 65, p. 691.
52. Hamu, G.B., Eliezer, D., and Wagner, L., *J. Alloy Compd.*, 2009, vol. 468, p. 222.
53. Kutniy, K.V., Papirov, I.I., Tikhonovsky, M.A., Pikalov, A.I., et al., *Mater. Sci. Eng. Technol.*, 2009, vol. 40, p. 242.
54. Song, D., Ma, A., Jiang, J., Lin, P., et al., *Corros. Sci.*, 2010, vol. 52, p. 481.
55. Song, D., Ma, A.B., Jiang, J.H., Lin, P.H., et al., *Corros. Sci.*, 2011, vol. 53, p. 362.
56. Li, N., Li, Y.D., Li, Y.X., Wu, Y.H., et al., *Mater. Sci. Eng., C*, 2014, vol. 35, p. 314.
57. Zhang, X., Yuan, G., and Wang, Z., *Mater. Lett.*, 2012, vol. 74, p. 128.
58. Wu, Q., Zhu, S., Wang, L., Liu, Q., et al., *J. Mech. Behav. Biomed. Mater.*, 2012, vol. 8, p. 1.
59. Zhang, X., Wang, Z., Yuan, G., and Xue, Y., *Mater. Sci. Eng., B*, 2012, 177, p. 1113.
60. Ralston, K.D. and Birbilis, N., *Corrosion*, 2010, vol. 66, p. 1.
61. Seong, J.W. and Kim, W.J., *Acta Biomater.*, 2015, vol. 11, p. 531.
62. Kim, H.S. and Kim, W.J., *Corros. Sci.*, 2013, vol. 75, p. 228.
63. Cao, F., Shi, Z., Song, G.L., Liu, M., et al., *Corros. Sci.*, 2015, vol. 90, p. 176.

64. Argade, G.R., Panigrahi, S.K., and Mishra, R.S., *Corros. Sci.*, 2012, vol. 58, p. 145.
65. Orlov, D., Ralston, K.D., Birbilis, N., and Estrin, Y., *Acta Mater.*, 2011, vol. 59, p. 6176.
66. Zhou, Y.-L., Li, Y., Luo, D.-M., Ding, Y., and Hodgson, P., *Mater. Sci. Eng., C*, 2015, vol. 49, p. 93.
67. Kim, H.S., Kim, G.H., Kim, H., and Kim, W.J., *Corros. Sci.*, 2013, vol. 74, p. 139.
68. Han, G., Lee, J.-Y., Kim, Y.-C., Park, J.H., et al., *Corros. Sci.*, 2012, vol. 63, p. 316.
69. Song, G.L. and Xu, Z., *Corros. Sci.*, 2012, vol. 54, p. 97.
70. Xin, R., Li, B., Li, L., and Liu, Q., *Mater. Des.*, 2011, vol. 32, p. 4548.
71. Song, G.L., Mishra, R., and Qing, X.Z., *Electrochem. Commun.*, 2010, vol. 12, p. 1009.
72. Song, G.L. and Xu, Z., *Corros. Sci.*, 2012, vol. 63, p. 100.
73. McCall, C.R., Hill, M.A., and Lillard, R.S., *Corros. Eng. Sci. Technol.*, 2005, vol. 40, p. 337.
74. Kim, H.S. and Kim, W.J., *Corros. Sci.*, 2013, vol. 75, p. 228.
75. Pu, Z., Song, G.L., Yang, S., Outeiro, J.C., et al., *Corros. Sci.*, 2012, vol. 57, p. 192.
76. Denkena, B. and Lucas, A., *CIRP J. Manuf. Sci. Technol.*, 2007, vol. 56, p. 113.
77. Harandi, S.E., Idris, M.H., and Jafari, H., *Mater. Des.*, 2011, vol. 32, no. 5, p. 2596.
78. Zhang, T., Shao, Y., Meng, G., Cui, Z., et al., *Corros. Sci.*, 2011, vol. 53, p. 1960.
79. Naing, A.N. and Zhou, W., *Corros. Sci.*, 2010, vol. 52, p. 589.
80. Zou, G., Peng, Q., Wang, Y., and Liu, B., *J. Alloy Compd.*, 2015, vol. 618, p. 44.
81. Somekawa, H. and Mukai, T., *Mater. Lett.*, 2012, vol. 76, p. 32.
82. Liu, Z.Y., Li, X.G., Du, C.W., Lu, L., et al., *Corros. Sci.*, 2009, vol. 51, p. 895.
83. Mostaed, E., Vedani, M., Hashempour, M., and Bestetti, M., *Biomaterials*, 2014, vol. 4, p. 1.
84. Zhang, X., Yuan, G., and Wang, Z., *Mater. Lett.*, 2012, vol. 74, p. 128.
85. Bobby Kannan, M., Dietzel, W., and Zettler, R., *J. Mater. Sci. Mater. Med.*, 2011, vol. 22, p. 2397.
86. Penga, Q., Lia, X., Maa, N., Liua, R., et al., *J. Mech. Behav. Biomed. Mater.*, 2012, vol. 10, p. 128.
87. Zhang, X., Yuan, G., Niu, J., Fu, P., et al., *J. Mech. Behav. Biomed. Mater.*, 2012, vol. 9, p. 153.
88. Jeong, Y.S. and Kim, W.J., *Corros. Sci.*, 2014, 82, p. 392.
89. Argade, J.R., Kandasamy, K., Panigrahi, S.K., and Mishra, R.S., *Corros. Sci.*, 2012, vol. 58, p. 321.